Blob-Representation of Multidimensional Objects and Surfaces

Edgar Garduño and Gabor T. Herman
Department of Computer Science
The Graduate Center
City University of New York

Presentation Outline

- Reconstruction from Projections: Series Expansion Methods.
- Selection of basis functions for Reconstruction.
- Selection of basis functions for Visualization.
- Raycasting for Implicit Surfaces.

Reconstruction from Projections

- Fourier Transform Methods. Based on the Central Slice Theorem.
- Series Expansion Methods. We assume that a density function υ can be represented by a linear combination of known basis functions, b_j:

$$\upsilon(\bar{x}) = \sum_{j=1}^{J} c_j b_j(\bar{x}), \quad \bar{x} \in \mathbb{R}^3$$

  - The set $\{c_j\}$, the *set of coefficients*, has to be determined by the reconstruction algorithm.
  - We refer to the set of points $\{\bar{p}_j\}$ to which the centers of the basis functions are located as a *grid*.

Transmission Electron Microscope

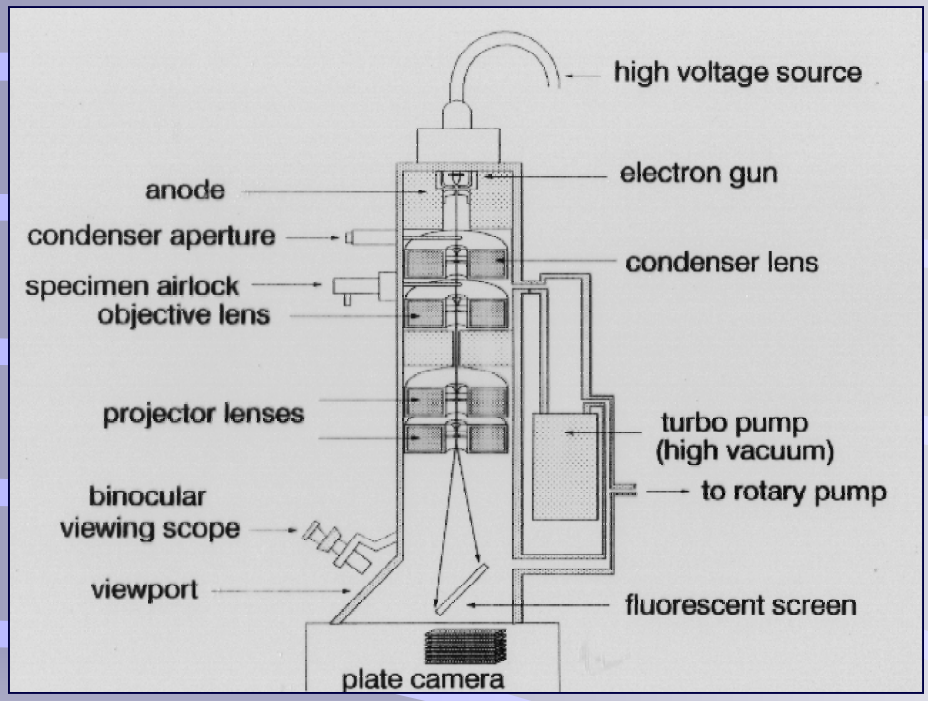

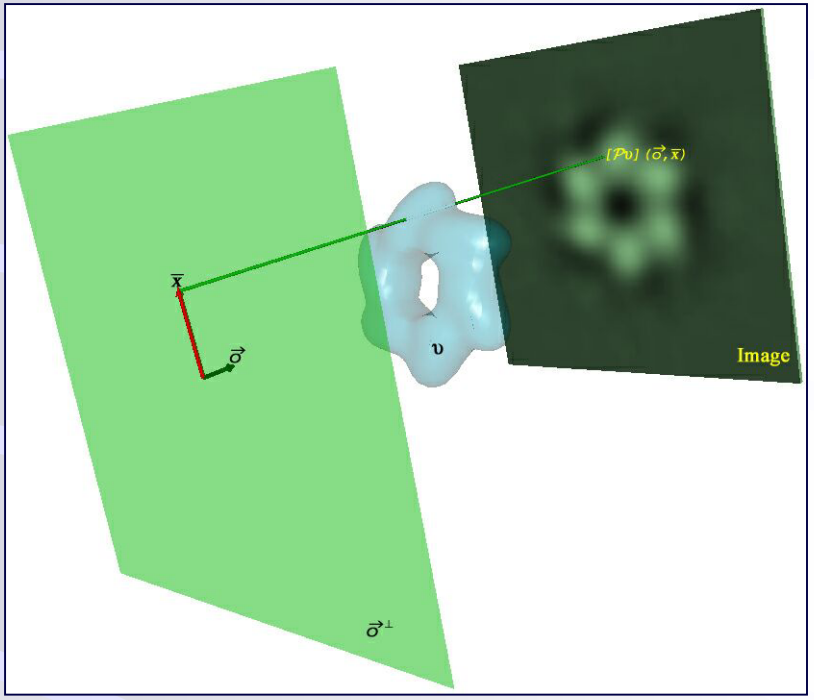

$$[\mathcal{P}\upsilon](\vec{o},\vec{x}) \approx \sum_{j=1}^{J} c_j [\mathcal{P}b_j](\vec{o},\vec{x})$$

$$y_i \approx \sum_{j=1}^{J} l_{i,j} c_j$$

Micrographs (Projections)

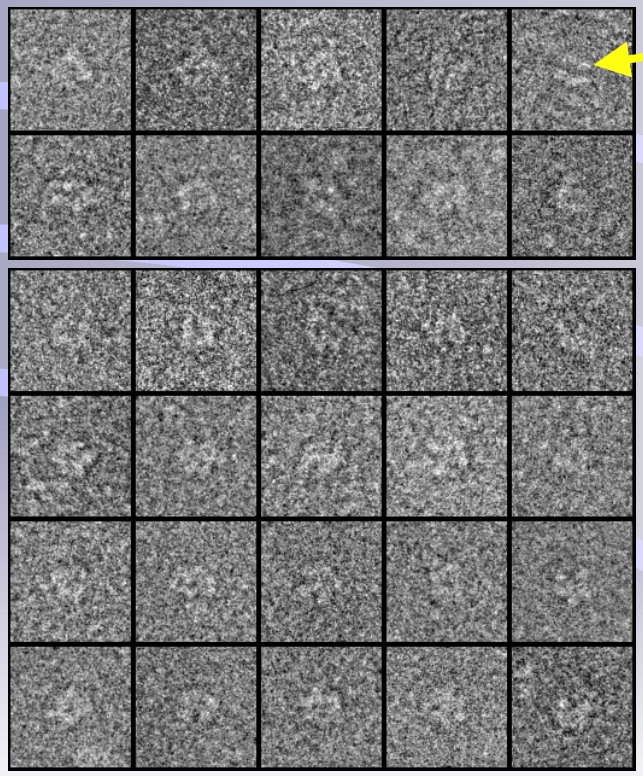

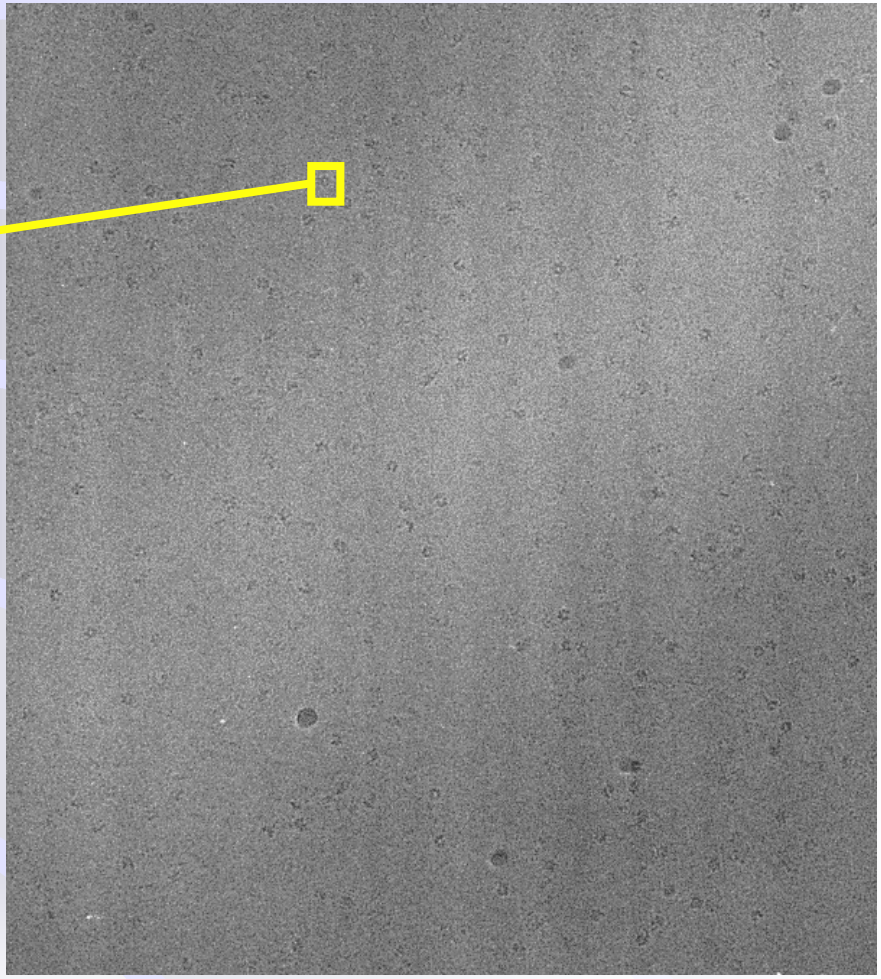

Block-ART

$$\bar{c}^{(k+1)} = \bar{c}^{(k)} + \lambda^{(k)} \sum_{i=(n-1)M+1}^{nM} \frac{y_i - \left\langle \bar{l}_i, \bar{c}^{(k)} \right\rangle}{\sum_{j=1}^{J} l_{i,j}^2} \bar{l}_i, \quad \text{for } n = \left[k \left(\text{mod } N \right) \right] + 1$$

N is the number of micrographs

M is the number of rays in each

Implementation using *footprints*

Selection of Basis Functions

- The choice of the set of basis functions $\{b_j\}$ greatly influences the result of the reconstruction algorithm.
- A common choice for basis functions are functions that have a unit value inside a cube and zero outside. However, the resulting approximation to υ is a piecewise constant function that has undesirable artificial sharp edges (biological objects are smooth).
- A better choice would be functions with a smooth transition from one to zero. We use basis functions, called *blobs*, with spherical symmetry and a smooth transition from one to zero

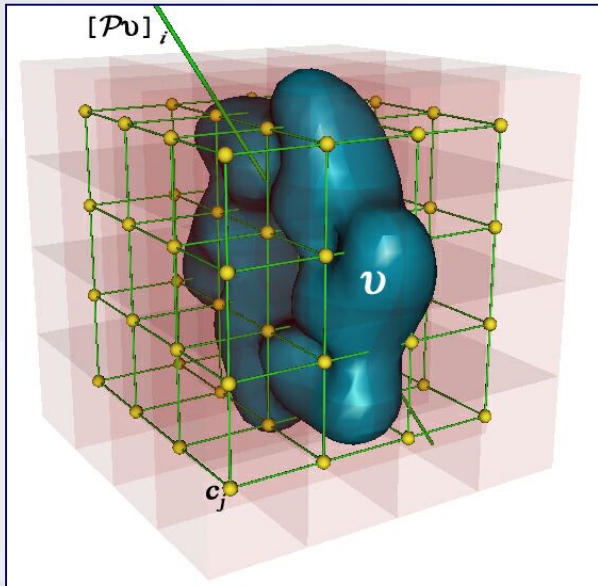

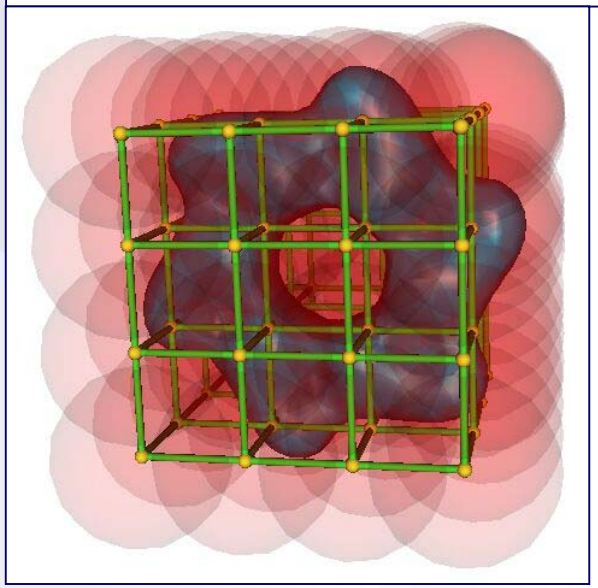

Generalized Kaiser-Bessel Functions (*blobs*)

- Blobs are generalizations of well-known window functions in digital signal processing called *Kaiser-Bessel*. The individual basis functions b_j are shifted versions of the blob defined by

$$b(m,\alpha,a;r)=\begin{cases}\dfrac{I_m\left(\alpha\sqrt{1-\left(\frac{r}{a}\right)^2}\right)}{I_m(\alpha)}\left(\sqrt{1-\left(\frac{r}{a}\right)^2}\right)^m, & \text{if } 0\le r\le a,\\ 0, & \text{otherwise,}\end{cases}$$

- m continuously differentiable (2 in our applications),
- Parameter α controls the width of the bell-shaped peak,
- Finite support (parameter a) and bandlimited (in practice).

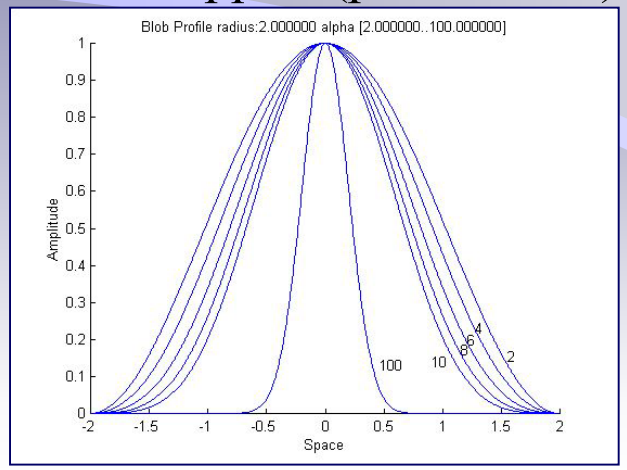

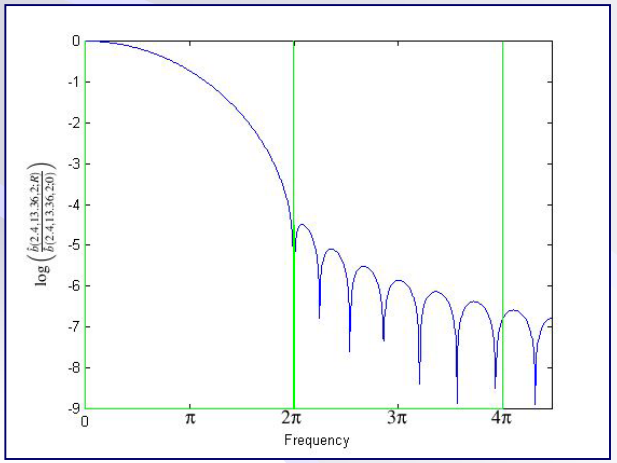

Grids for Blob Centers

We consider three different grids:

Simple Cubic Grid
(*sc*)

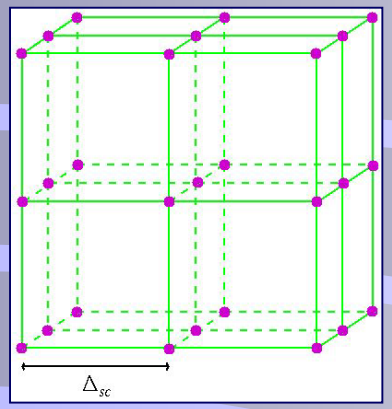

$$G_\Delta = \left\{ \Delta\bar{k} \;\middle|\; \bar{k} \in \mathbb{Z}^3 \right\}$$

Body-Center Cubic Grid
(*bcc*)

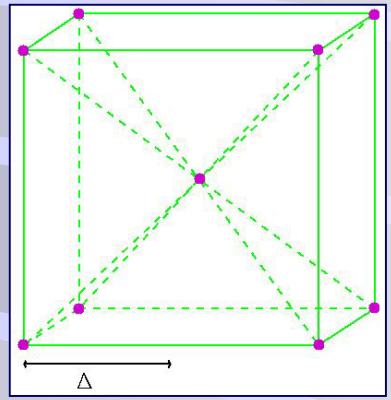

$$B_\Delta = \left\{ \Delta\bar{k} \;\middle|\; \bar{k} \in \mathbb{Z}^3 \text{ and } k_1 \equiv k_2 \equiv k_3 \pmod 2 \right\}$$

Face-Centered Cubic Grid
(*fcc*)

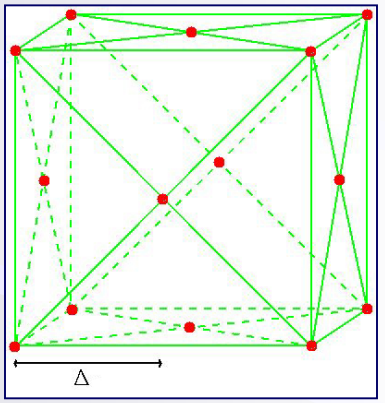

$$F_\Delta = \left\{ \Delta\bar{k} \;\middle|\; \bar{k} \in \mathbb{Z}^3 \text{ and } k_1 + k_2 + k_3 \equiv 0 \pmod 2 \right\}$$

Blobs and Grid Spacing

- It is important to determine the distance between grid points (Δ) as well as a and α. A reasonable criterion is provided by the representation of a constant-valued density function by a linear combination of blobs.
- Convolution: $[f * g](\bar{x}) = \int_{\mathbb{R}^3} f(\bar{x} - \bar{y}) g(\bar{y}) d\bar{y}$
- Sampling: The *Dirac* function δ (a tempered distribution) is defined by:

$$\delta f = f(\bar{0}).$$

Let $f_{\bar{y}}$ denote the function $f_{\bar{y}}(\bar{y}) = f(\bar{x} - \bar{y})$. Thus, we can extend this definition to the *Dirac* function as follows:

$$\delta_{\bar{y}} f = f(\bar{y}).$$

We can express a *train of pulses* on the grid G_Δ as follows:

$$^{\Delta}shah = \sum_{\bar{y} \in G_\Delta} \delta_{\bar{y}} \longrightarrow \text{Ш}_{G_\Delta} = {}^{\Delta}shah.$$

Sampling a function f over the simple cubic grid is defined by

$$\text{Ш}_{G_\Delta} \times f = \sum_{\bar{y} \in G_\Delta} f(\bar{y}).$$

Train of pulses can be generalized to the B_Δ and F_Δ grids by:

$$\text{Ш}_{B_\Delta} = {}^{2\Delta}shah + {}^{2\Delta}shah_{\bar{b}}$$

$$\text{Ш}_{F_\Delta} = {}^{2\Delta}shah + {}^{2\Delta}shah_{\bar{e}_0} + {}^{2\Delta}shah_{\bar{e}_1} + {}^{2\Delta}shah_{\bar{e}_2}$$

Relationship between a, α and Δ (part 1)

- With c_j=1, for $1 \le j \le J$, should be an approximation of a constant valued function. Thus, the approximation is defined by:

$$\sum_{j=1}^{J} b_j = b * \mathrm{III}_{B_\Delta},$$

by the convolution Theorem we have:

$$\widehat{b * \mathrm{III}_{B_\Delta}} = \hat{b} \times \widehat{\mathrm{III}_{B_\Delta}}.$$

We define the Fourier transform of a function g by:

$$g(\bar{\xi}) = (2\pi)^{-\frac{n}{2}} \int_{\mathbb{R}^n} g(\bar{x}) e^{-i\langle \bar{x}, \bar{\xi} \rangle} d\bar{x},$$

under this definition is easy to prove that:

$$\widehat{\mathrm{III}_{B_\Delta}} = \frac{1}{\sqrt{2}} \left(\frac{\sqrt{\pi}}{\Delta} \right)^3 \mathrm{III}_{F_{\frac{\pi}{\Delta}}}.$$

- More about blobs. The analytical Fourier transform of 3-dimensional blobs is defined by

$$\hat{b}(2,\alpha,a;R) = \frac{a^3 \alpha^2}{I_2(\alpha)} \begin{cases} \dfrac{I_{\frac{7}{2}}\left(\sqrt{\alpha^2 - (aR)^2}\right)}{\left(\sqrt{\alpha^2 - (aR)^2}\right)^{\frac{7}{2}}}, & \text{if } aR \le \alpha \\ \dfrac{J_{\frac{7}{2}}\left(\sqrt{(aR)^2 - \alpha^2}\right)}{\left(\sqrt{(aR)^2 - \alpha^2}\right)^{\frac{7}{2}}}, & \text{if } aR \ge \alpha \end{cases}$$

Relationship between a, α and Δ (part 2)

- The Fourier transform of a constant valued function is an impulse centered at the origin. Therefore, for $\hat{b} \times \frac{1}{\sqrt{2}} \left(\frac{\sqrt{\pi}}{\Delta} \right)^3 \text{Ш}_{F_{\frac{\pi}{\Delta}}}$ to best approximate the Fourier transform of a constant-valued function it is useful to select b in such a way that $\hat{b}(2, \alpha, a; R)$ is zero-valued at the locations of F which have the smallest positive distance from the origin; i.e., at the frequency $R = \frac{\sqrt{2}\pi}{\Delta}$. Since $I_{\frac{7}{2}}$ is not zero-valued and the smallest positive x for which $J_{\frac{7}{2}}(x) = 0$ is $x = 6.987932$, it follows

$$\alpha = \sqrt{2\pi^2 \left(\frac{a}{\Delta} \right)^2 - 6.987932^2}$$

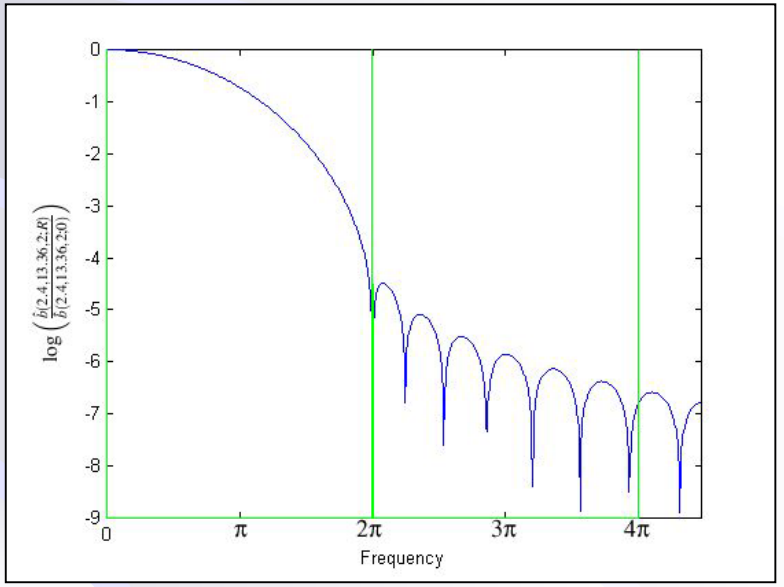

Optimized Parameters for Reconstruction

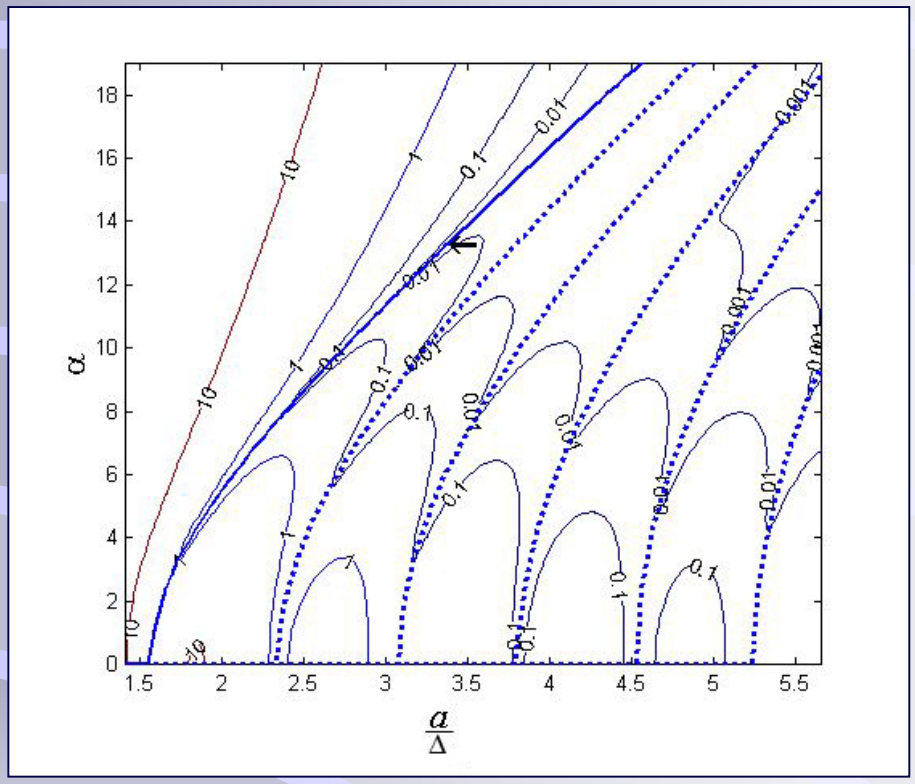

The root mean square (*rms*) error between a constant-valued function and its approximation by a linear combination of blobs using several values α and $\frac{a}{\Delta}$ (with $\Delta = \frac{1}{\sqrt{2}}$)

Implicit Surfaces

- An implicit surface (also called isosurfaces or isointensity surfaces) is defined as a set of points in space such that

$$S = \left\{ (\bar{x}) \middle| \upsilon(\bar{x}) = t \right\}$$

- The assumption is that there is a threshold t such that the object of interest consists of exactly those points at which the value of υ is greater than the threshold. If the total volume of the object of interest is known (as is the case in some applications, such as electron microscopy), then t is uniquely determined by the criterion that S should enclose exactly the known volume. For visualization of the object of interest it is then sufficient to display its surface S.
- These are appropriate for objects with complex topologies and geometries such as organic objects or man-made shapes and therefore have been used to visualize objects of interest in many areas of science.
- A standard way of specifying a density function υ is by a linear combination of basis functions, exactly as in the series expansion methods.

$$S = \left\{ (\bar{x}) \middle| \upsilon(\bar{x}) = \sum_{j=1}^{J} c_j b_j (\bar{x}) = t \right\}$$

Implicit Surfaces and Raycasting

- Visualizing implicit surfaces can be performed by polygonization or direct ray tracing.

- Implicit surfaces are particularly well suited for ray-intersection processing: the density function defining the implicit surface enables us to compute the intersection between a ray and the surface by standard numerical zero-finding methods.

- In one of its forms raycasting consists of casting a finite number of rays perpendicular to the computer screen towards *S*.

- In general, raycasting is slower than the polygon-projection methods. However, an accurate visualization of an implicit surface requires a careful selection of polygons, something that is avoided by raycasting whose accuracy is automatically determined by the pixel locations on the computer screen.

Raycasting with blobs

- The representation of an implicit surface, approximated by a linear combination of blobs, by raycasting would be an accurate representation of the reconstructed volume, only limited by the reconstruction and thresholding processes.

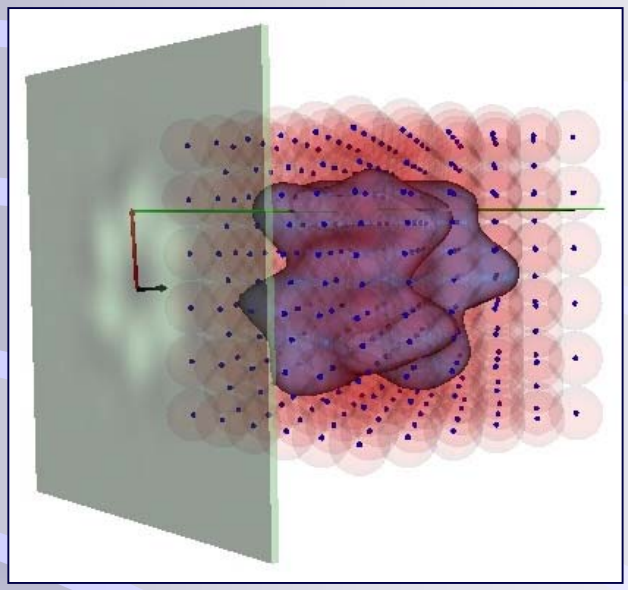

- The visualization based on the linear combination of blobs should produce a surface with accurate normals as we have analytical formulas for ∇b_j:

$$\nabla \upsilon(\bar{x}) = \sum_{j=1}^{J} c_j \nabla b_j(\bar{x})$$

Implicit Surface of Complex DnaB·DnaC After Reconstruction

- In the field of electron microscopy of biological macromolecules, the threshold can be obtained by combining the knowledge of the molecular weight of a protein and the volume occupied in a voxel in the voxelized version of $\upsilon(\bar{x})$.
- Interestingly, not all the "good" blobs used for reconstructing will produce good results when the implicit surface of a reconstruction is visualized. For example:

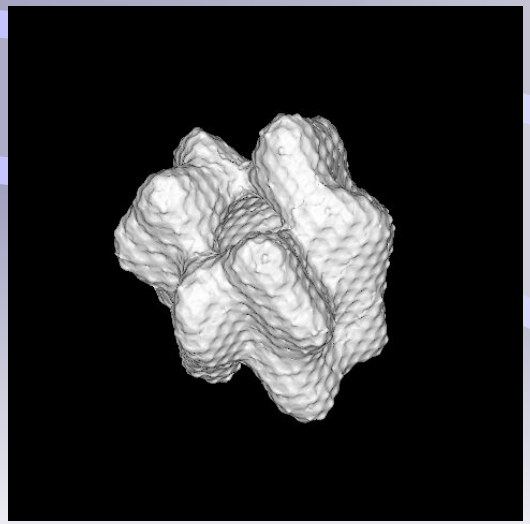

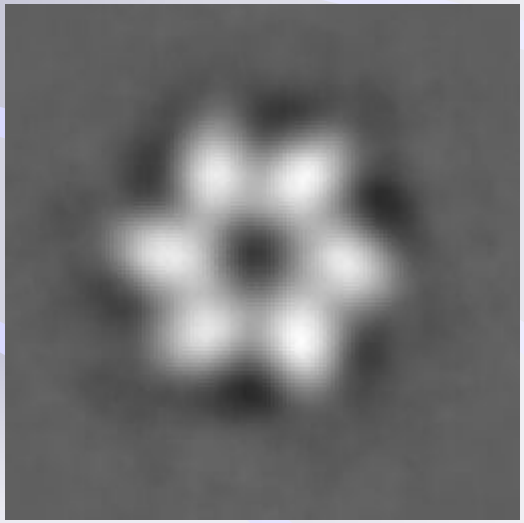

Reconstruction Parameters:

$a = 1.25,\ \alpha = 3.6$

$$\Delta = \frac{1}{\sqrt{2}}$$

Impact of a, α and Δ on the Final Surface

- Unfortunately, only a handful of proteins are well-known.
- Reconstruction of a well-known object.

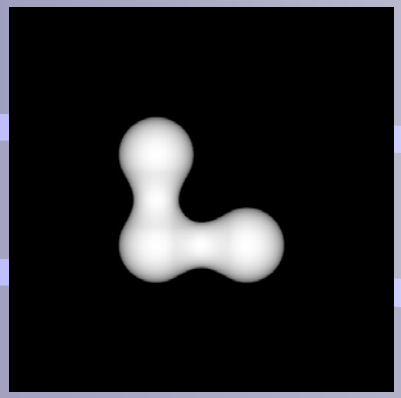
a=1.25, α=3.60

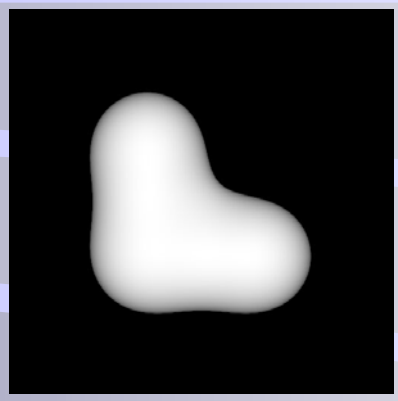
a=2.40, α=13.36

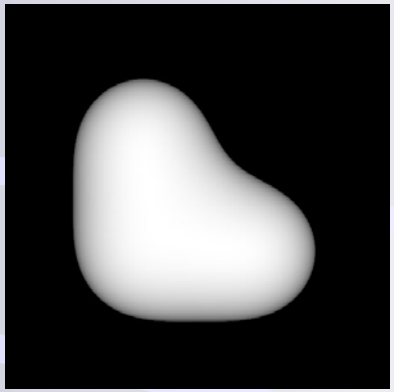
a=3.20, α=18.85

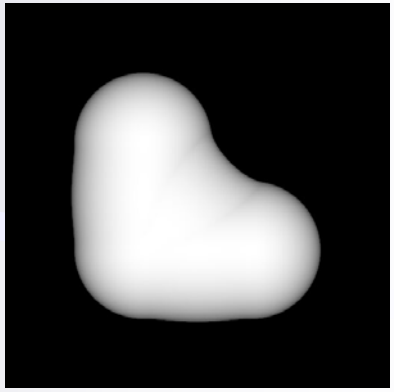
a=1.65, α=0.00

First zero

Second zero

- The ratio a/Δ should be neither too small (artifacts) nor too large (blurring).

Convexity Between 2 Closest Neighbors

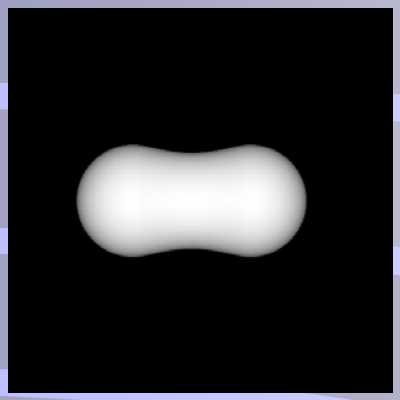
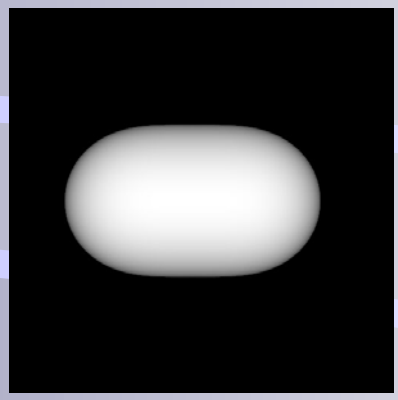
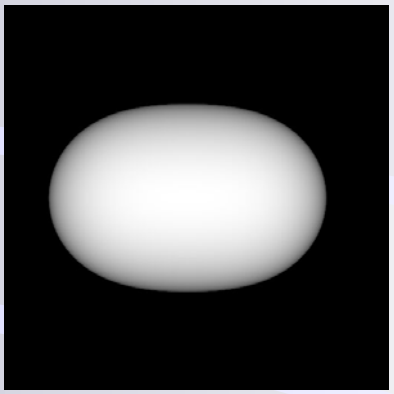
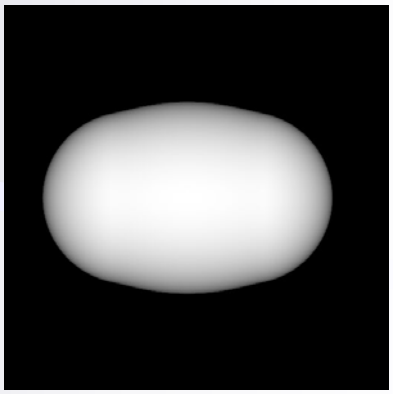

a=1.25, α=3.60 a=2.40, α=13.36 a=3.20, α=18.85 a=1.65, α=0.00

First zero Second zero

- We propose the following criterion to make a definite choice of a, α and Δ: if two blobs at nearest grid points in the grid B_Δ are given coefficients 1 with all other blobs given coefficients 0, then the implicit surface thresholded at $t = 0.5$ should enclose a minimum volume convex set.

Definite choice of Blob Parameters

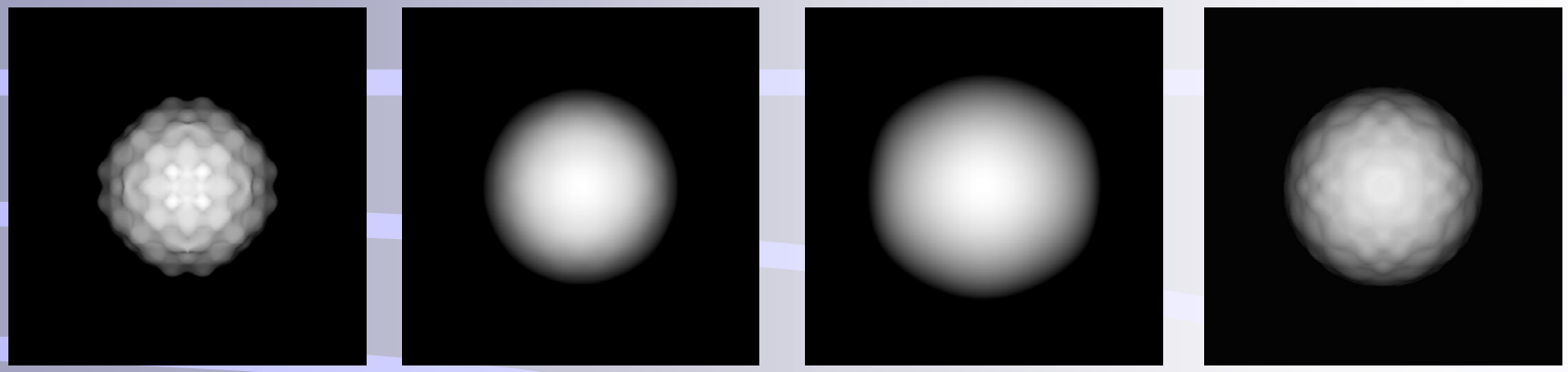

a=1.25, α=3.60 *a*=2.40, α=13.36 *a*=3.20, α=18.85 *a*=1.65, α=0.00

First zero Second zero

- We evaluated the resulting error between a surface and its approximation, as measured by the difference between the surface normals. For this test we selected a distribution υ_s with a constant value 1 inside a sphere and 0 outside.
- For each set $\{c_j\}$ produced by the reconstruction algorithm, raycasting was used to create a visualization of the implicit surface of the reconstructed sphere at threshold 0.5.

Optimized Parameters for Visualization

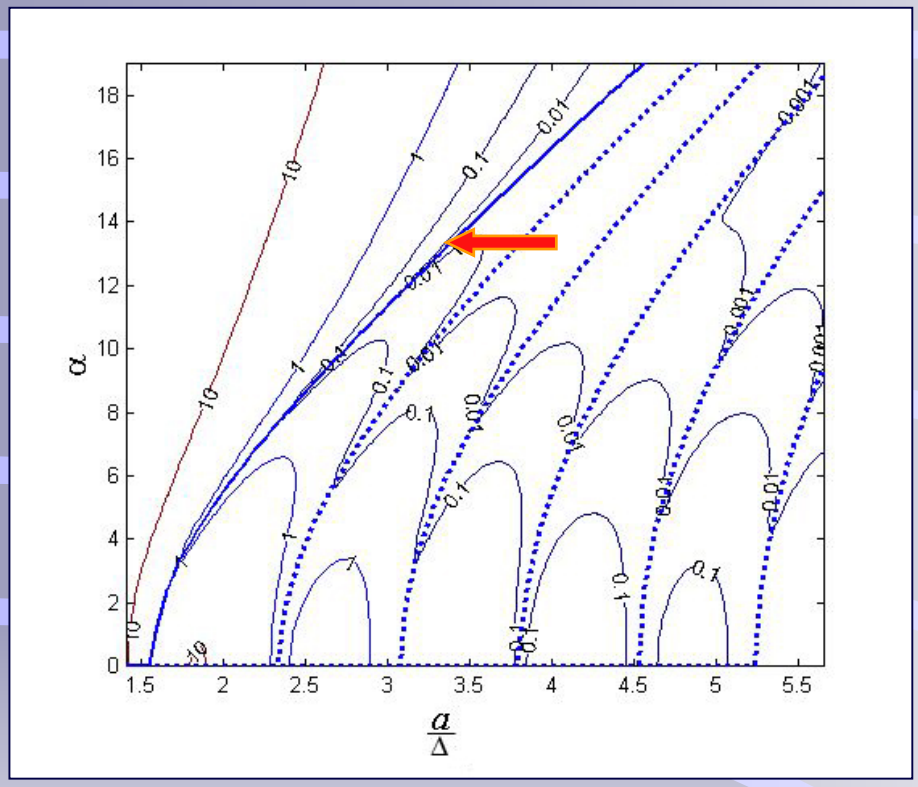

The root mean square (rms) error between a constant-valued function and its approximation by a linear combination of blobs using several values α and $\frac{a}{\Delta}$ (with $\Delta = \frac{1}{\sqrt{2}}$)

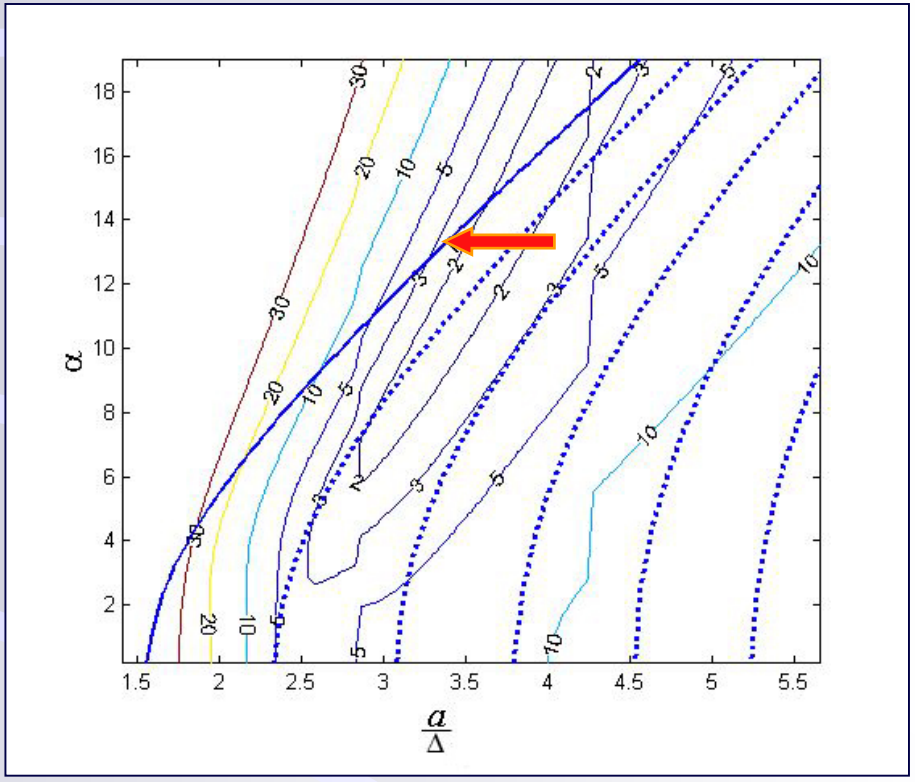

The root mean square (rms) error between analytic normals to a sphere and normals to the implicit surface of its reconstruction at each display point for which the ray casted crosses both surfaces

Visual Results

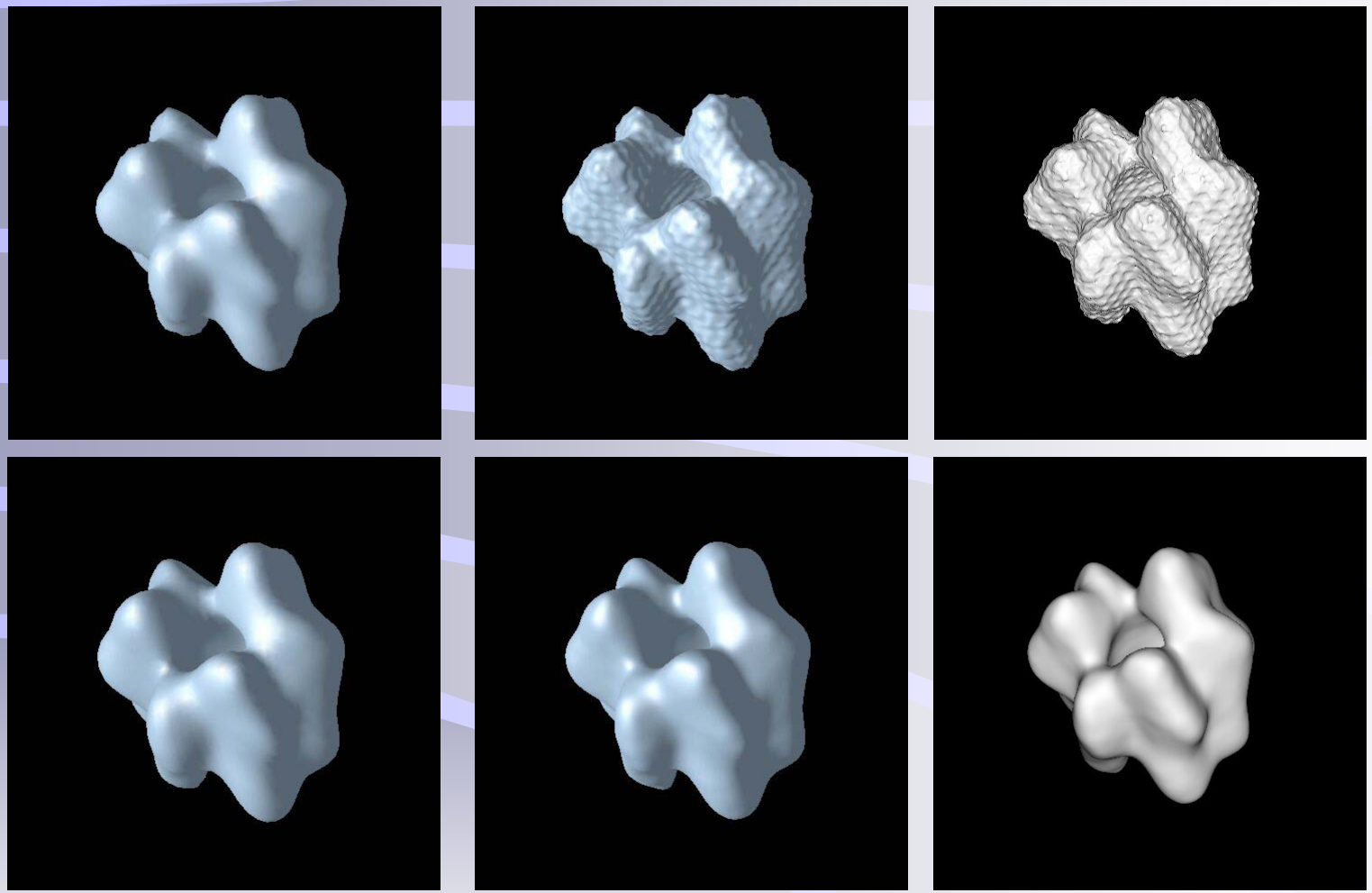

a=1.25

α=3.60

a=2.40

α=13.36

128 ×128 ×128

400×400×400

OpenDX

Raycasting

Raycasting-Blobs

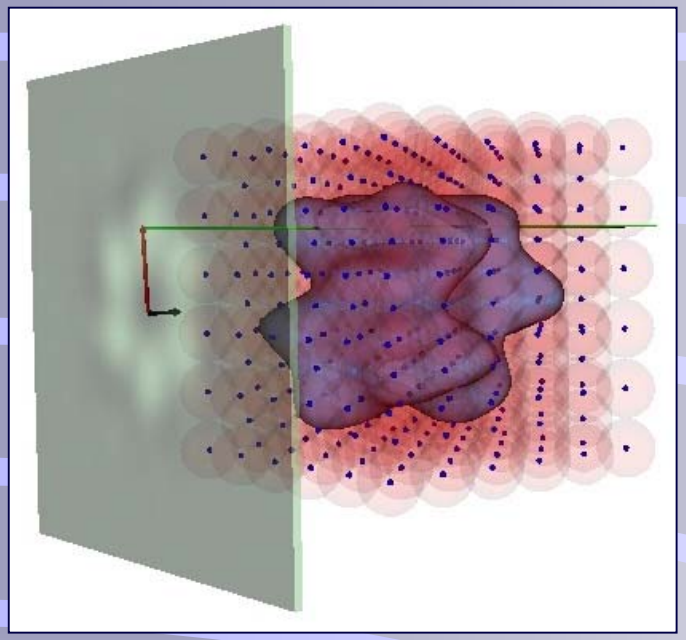

General Scheme

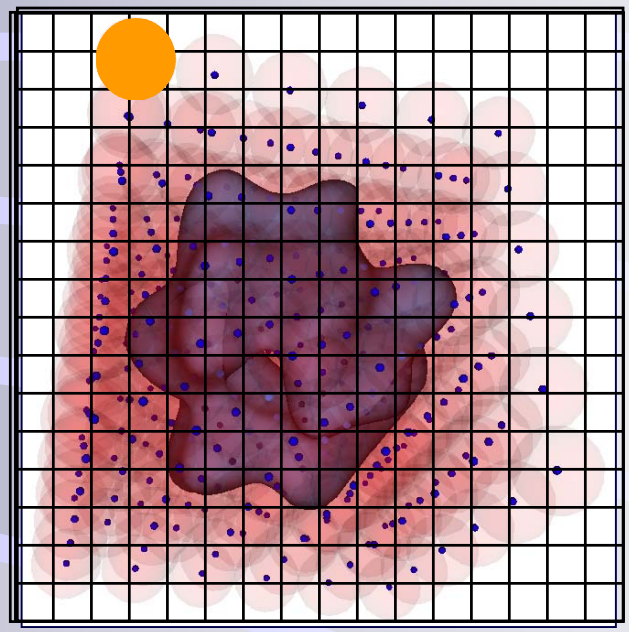

Projection of Shadows

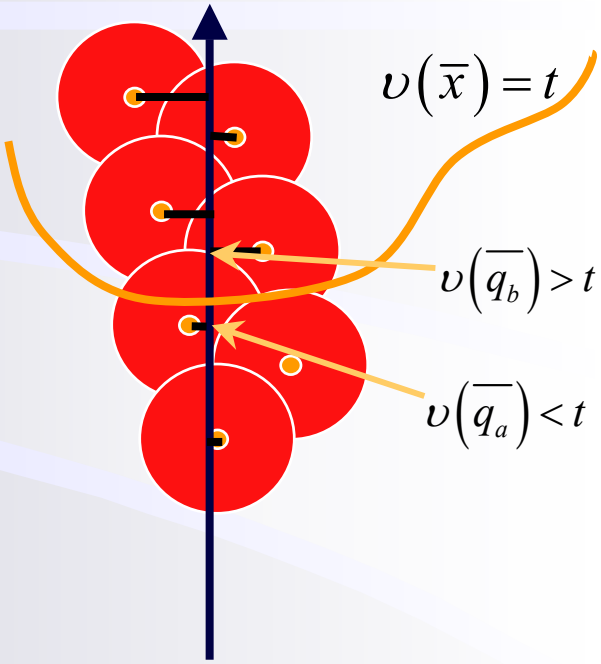

Plane

Too slow for real-time user interaction

Improvements to Raycasting-blobs Method

Restrict the search to those c_js that contribute to the formation of the object of interest.

Use a discretized version of υ evaluated over the points $\{\overline{p_j}\}$ defined as v_j.

Find an estimate to where the points $\overline{q_a}$ and $\overline{q_b}$ are.

Z-buffer algorithm using the set v_j and the shadows of the blobs.

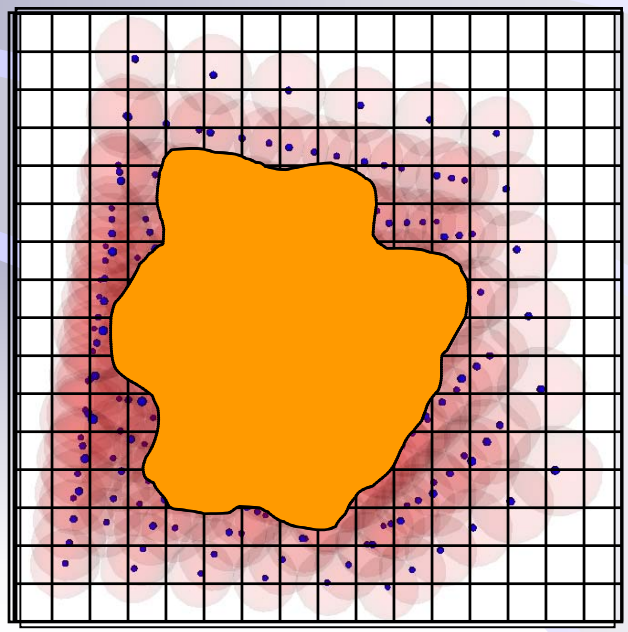

Results of Improved Raycasting-blobs Method

Reduction of computing time by 20 times preserving image quality

Not Real-time

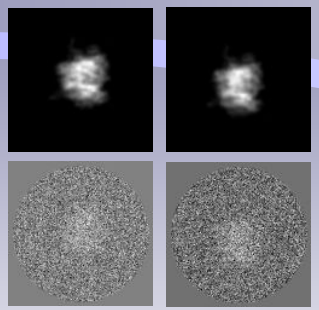

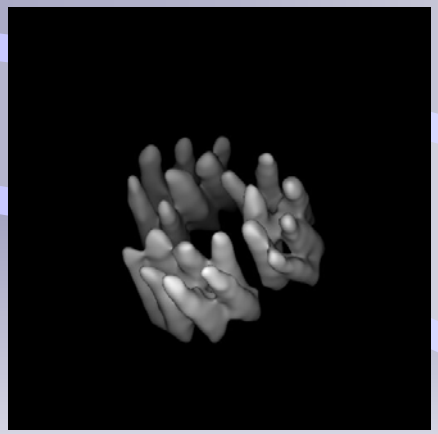

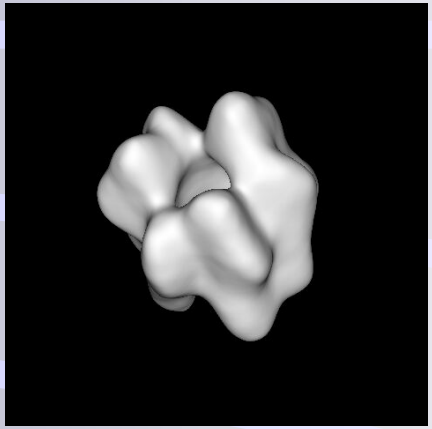

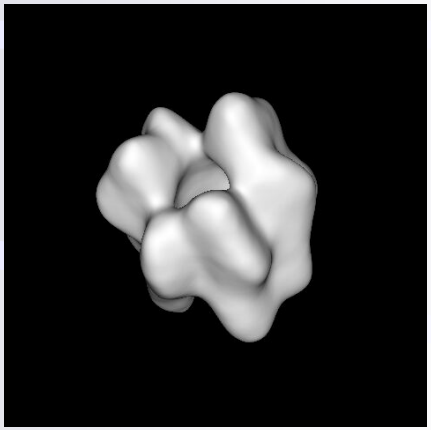

DnaB·DnaC

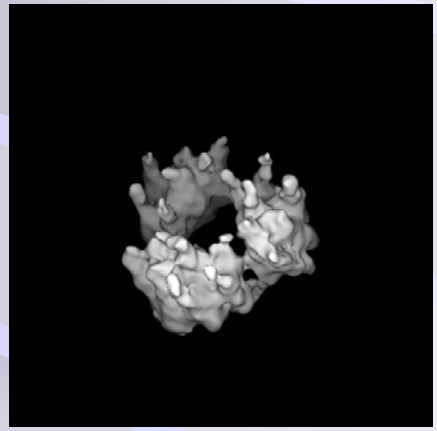

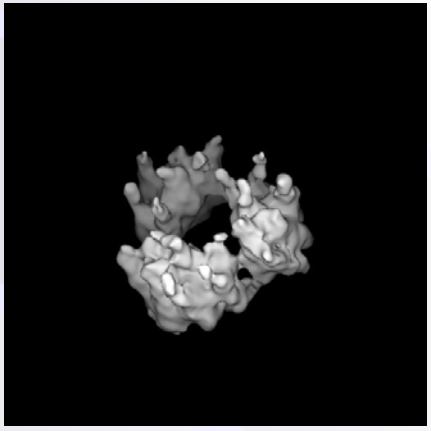

Bacterio-rhodopsin

Projections

"truth"

1.5 hrs

~200 s

References for Further Reading

- J. F. Blinn, "A generalization of algebraic surface drawing," *ACM Transactions on Graphics*, vol. 1, pp. 235-256, 1982.
- J. Bloomenthal, *Introduction to Implicit Surfaces*. San Francisco: Morgan Kaufmann, 1997.
- H. Q. Dinh, G. Turk, and G. Slabaugh, "Reconstructing surfaces by volumetric regularization using radial basis functions," *IEEE Transactions On Pattern Analysis and Machine Intelligence*, vol. 24, pp. 1358-1371, 2002.
- E. Garduño and G. T. Herman, "Optimization of basis functions for both reconstruction and visualization," *Discrete Applied Mathematics*, to appear.
- R. M. Lewitt, "Multidimensional digital image representations using generalized Kaiser-Bessel window functions," *Journal of the Optical Society of America A: Optics, Image Science, and Vision*, vol. 7, pp. 1834-1846, 1990.
- R. Marabini, G. T. Herman, and J. M. Carazo, "3D reconstruction in electon microscopy using ART with smooth spherically symmetric volume elements (blobs)," *Ultramicroscopy*, vol. 15, pp. 68-78, 1996.
- S. Muraki, "Volumetric shape description of range data using ”Blobby Model”," *Computer Graphics*, vol. 25, pp. 227–235, 1991.
- M. Zwicker, H. Pfister, J. van Baar, and M. Gross, "EWA splatting," *IEEE Transactions on Visualization and Computer Graphics*, vol. 8, pp. 223–238, 2002.